arXiv:1109.3518v2 [physics.optics] 19 Sep 2011

Tuning the Nonlinear Response of Coupled Split-Ring Resonators

Kirsty E. Hannam, David A. Powell, Ilya V. Shadrivov, and Yuri S. Kivshar
Nonlinear Physics Centre, Research School of Physics and Engineering, The Australian National University, Canberra ACT 0200, Australia

We introduce the concept of controlling the nonlinear response of the metamaterial by altering its internal structure. We experimentally demonstrate that we can tune the nonlinear frequency shift for two coupled split-ring resonators by changing their mutual position. This effect is achieved through modification of the structure of the coupled resonant modes and their interaction with the incident field. We explain these results with the aid of numerical modeling, which shows that by offsetting the resonators we control the maximum currents through the nonlinear driving elements which affects the nonlinear response of the system.

The concept of engineering the electromagnetic properties of a material to possess a negative refractive index was first put forward by Veselago in 1968[1]. The first experimental confirmation of this idea was accomplished by Smith *et al.* in 2000[2], using a metamaterial consisting of a combination of split-ring resonators (SRRs) to provide a negative permeability[3], and thin metal wires to provide a negative permittivity. More recently, metamaterials composed of only SRRs have been used to produce optical activity[4], offering an alternate route to negative refraction[5].

The effective properties of these metamaterials depend both on the properties of the individual SRRs, and on the arrangement of the SRRs in the lattice, as strong interactions occur between the rings in a lattice due to their complex near-field patterns. This allows us to significantly control the properties of the metamaterial by changing the internal structure of the composite material[6]. In order to understand the resulting responses of the metamaterial, we need to understand the interactions between the individual SRRs. This is a major motivation behind the studies involving the relative positions of two SRRs, including rotating them[7], and shifting them with respect to each other[8].

The linear properties of individual metamaterial elements can also be controlled by an external signal, by inserting *nonlinear inclusions* such as semiconductors[9] or diodes[10] into the rings. Many tunable inclusions can also respond to the high-frequency incident wave, thus they form the basis of *nonlinear metamaterials*, which typically have power-dependent resonant frequencies[11–14]. The nonlinear response of metamaterials can be much stronger than that of natural materials, due to their resonant nature, and the local field enhancement which occurs at certain "hot spots".

The strength of the local field depends on the design of the resonator, and the choice of an optimal location to place the nonlinear element. However it also depends strongly on the coupling of the wave to the external field, which along with losses determines the quality factor of the resonator. Since modifications of the lattice parameters also influence the quality factor of the resonances[8], they should affect the local-field enhancement. In this Letter we experimentally demonstrate, for the first time to our knowledge, *a control of the nonlinear response* of two broadside-coupled split-ring resonators by modifying the offset between them, and explain this response by studying how shifting the resonances changes the maximum currents in the resonators.

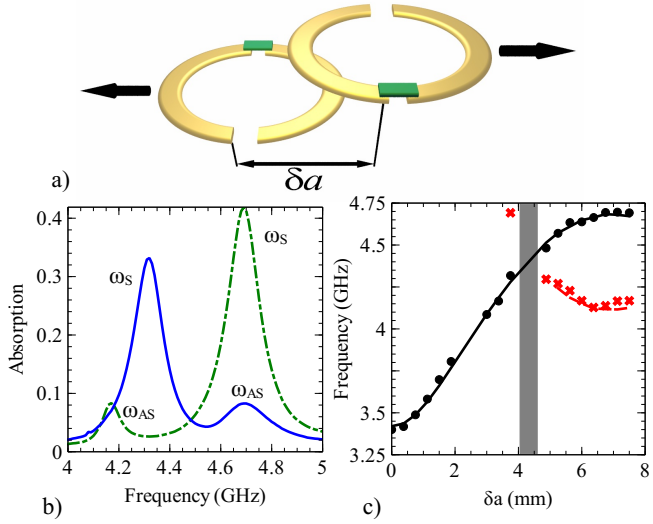

FIG. 1. (a) Schematic of the lateral shifting of SRRs with inserted diodes; δa is a shift between two rings. (b) The measured absorption curves for $\delta a = 3.75$ mm (blue solid) and 7.5 mm (green dashed), at -20dBm input power. Symmetric (ω_S) and antisymmetric (ω_{AS}) modes are highlighted. (c) Resonant frequencies of symmetric (black circle/solid) and antisymmetric (red cross/dashed) resonances, as determined both experimentally (markers) and numerically (lines) for the linear case.

First, we perform microwave experiments with a pair of SRRs, having an offset δa between their centers, as shown schematically in Fig. 1(a). The copper rings are 3.75 mm in outer radius, 3.25 mm in inner radius, and have a gap width of 1 mm. These rings are printed on the opposite sides of 1.6 mm thick FR4 circuit board. Each ring has a second gap of 0.4 mm opposite the first gap, across which a Skyworks SMV1405-079 series diode is soldered. The samples were placed inside WR-229 rectangular waveguide, oriented such that the incoming magnetic field is perpendicular to the loops.

The transmission and reflection from the sample are

measured using a Rohde and Schwarz ZVB-20 vector network analyzer. We measure the absorption spectrum, which describes the frequency of the maximum current distribution in the rings, given by $1 - |S_{21}|^2 - |S_{11}|^2$, where S_{21} and S_{11} are the transmission and reflection coefficients, respectively. The absorption curves are measured experimentally for the values of δa between 0 and 7.5 mm, in 0.375 mm increments, at powers -20 dBm and 15 dBm. Numerical results are calculated using CST Microwave Studio. Each diode is replaced by a series RLC circuit with 2.67 pF capacitor, 0.8Ω resistor and 0.7 nH inductor. Such a circuit describes the diode in the linear regime[15].

Figure 1(b) shows the measured absorption curves for δa equal to 3.75 mm, and 7.5 mm, at -20 dBm. There are seen clearly two resonant modes, symmetric and antisymmetric, which are defined by the relative directions of the currents on the rings. These modes are both tunable through a change of δa[6,8], which is evident, as when $\delta a = 3.75$ mm the symmetric (antisymmetric) mode is the lower (higher) resonant mode, while when $\delta a = 7.5$ mm it has increased (decreased) to become the higher (lower) resonant mode. The frequencies of maximum absorption for both modes are found and plotted as a function of δa in Fig. 1(c) (markers), along with the numerical equivalents (solid lines). We observe excellent agreement between the experimental and numerical results. Consistent with the findings in Ref. 8, there are strong responses in both the modes, with the resonant frequency of the symmetric mode increasing with an increase in δa.

As seen in Fig. 1(b), the symmetric mode is much more strongly excited than the antisymmetric mode. In fact, the antisymmetric mode is not visible for low values of δa, as seen in Fig. 1(c), as the coupling to the incident wave is very weak. However, we have enough points to see that the antisymmetric mode is still tunable via the lateral shifting.

In a single SRR, the resonant frequency is determined by $\omega = 1/\sqrt{LC}$, where L is inductance, and C is capacitance. Introducing the diode adds a nonlinear capacitance C_V in series with the capacitance of the SRR. By adding the second SRR, we introduce coupling between the rings, which causes a split in the resonant frequency, resulting in the two modes previously discussed, ω_S and ω_{AS}. By changing the intensity of the incoming microwaves, we are causing a nonlinear change in the capacitance of the diodes, which changes the effective capacitance of the system, and shifts the resonant frequencies. This results in having an added degree of freedom for manipulating our system.

In our structure, the nonlinear response is quantified by a shift of the resonant frequency with increasing input power from -20dBm to 15dBm. The relative difference between the low- and high-power resonant frequencies for each value of δa is shown in Fig. 2. The inset in Fig. 2 shows the absorption of the symmetric peak for both powers when $\delta a = 3.75$ mm. We observe a significant change of the nonlinear frequency shift as a function of the linear offset. It is clear that the nonlinearity is much stronger for the symmetric resonance when the rings are closer together. It can be seen that the antisymmetric mode is also tuned by the increasing power, though due to the excitation we use, we cannot excite this mode for smaller offsets.

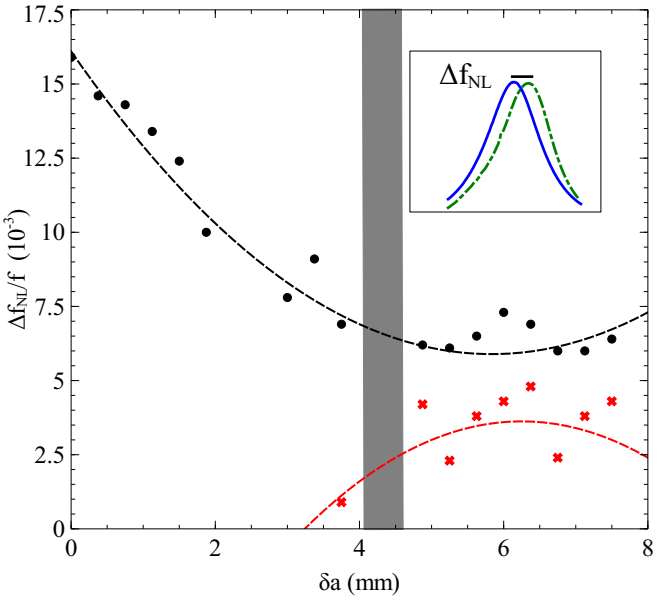

FIG. 2. Relative nonlinear shift in symmetric (black circles) and antisymmetric (red crosses) resonant frequencies for shifts (δa). The dashed lines are second order polynomial fits to the data. The inset shows the nonlinear shift of the absorption at the symmetric mode when $\delta a = 3.75$ mm. The solid blue line is at -20dBm, and the green dashed line at 15dBm.

We can explain the nonlinear tuning by looking both experimentally and numerically at some of the linear aspects of the system. As the nonlinear shift is due to the currents excited in the rings (which also leads to absorption), it would be expected the higher the absorption, the

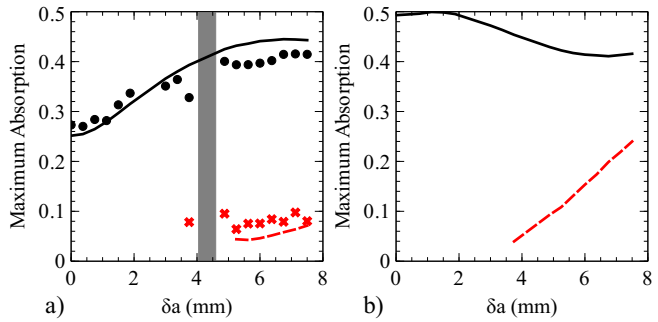

FIG. 3. (a) Experimental (markers) and numerical (lines) maximum absorptions for both symmetric (black circle/solid) and antisymmetric (red cross/dashed) modes. (b) Numerically calculated absorption coefficients at the resonant frequencies for the case of a lossless substrate.

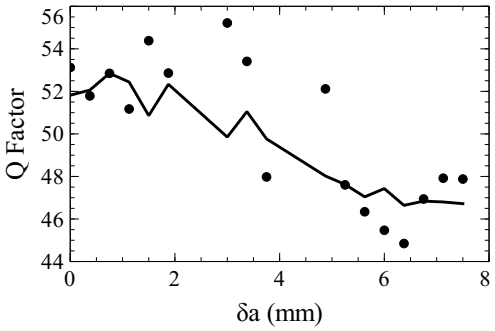

FIG. 4. Experimental (markers) and numerical (solid line) Q factors of the symmetric mode.

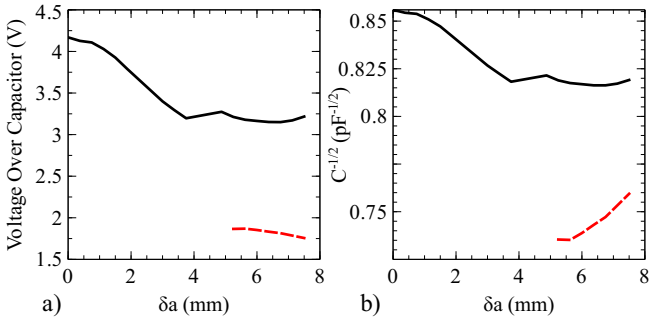

FIG. 5. (a) Calculated voltage over the capacitive component of the diode. (b) Resulting capacitance (presented as 1/sqrt(C)).

larger the nonlinear response. Therefore the maximum absorption for each value of δa is plotted in Fig. 3(a) for both modes, showing good agreement between experimental and numerical results. However, by comparing this figure with Fig. 2, we see *increasing absorption* with *decreasing nonlinear shift*. This effect appears due to the fact that, offsetting the rings, we not only modify the current amplitudes in the rings, but also change the field distribution in the substrate. As a result, the total absorption presented in Fig. 3(a) contains contribution from losses in both metal and in dielectric. At the same time, the nonlinear response in our case is caused by currents in metal only. The losses within the FR4 dielectric circuit board increase with δa due to increased field confinement within the board, and change in these losses dominate changes of the absorption in metal. In Fig. 3(b) we show the results of a simulation which neglects dielectric losses. We can see that these maxima now decrease as δa increases, agreeing with the trend in the nonlinear response. The difference in trends between Figs. 3(a & b) confirms explained above effect of dielectric losses.

The amplitude of the currents in the system depends on the Q factor of the resonator. Because of this we would expect to see some correlation between the changing nonlinear shift, and the Q factor. By comparing Fig. 2 with Fig. 4, where we have plotted the Q factor as a function of δa for the symmetric mode, we can see that this is indeed the case, and decreasing quality factor leads to the decrease of the nonlinear response.

The physics of the nonlinear shift of the resonant frequency was studied in Ref.[12], where it was shown that the rectified AC voltage across the varactor provides self-biasing mechanism. By increasing the amplitude of the electromagnetic wave, we increase alternating voltages in the SRR, generating a larger DC bias voltage, which reduces the varactor capacitance. To study this effect, we performed numerical simulations, and monitored the voltages on each RLC circuit representing a varactor. As a larger voltage leads to a stronger decrease in the varactor capacitance, we would expect to see a similar trend between the voltages recorded at the resonant frequency, and the nonlinear shift. We want to note that the voltage across the capacitance, and not the whole RLC circuit should be calculated. Corresponding DC voltage at the resonant frequency is plotted for both resonant modes in Fig. 5(a).

By comparing Figs. 2, 3(b), and 5(a), we can see an overall correlation, where as δa increases there is a decreasing trend in the nonlinear response, the maximum lossless absorptions, and the calculated voltages, for the symmetric mode. This enables us to explain the nonlinear response of the system in a meaningful way.

As the nonlinear response should be directly proportional to the inverse of the square root of the capacitance, we then calculated this capacitance using the known voltage across the diode. From the data sheets for the diode, we can obtain the capacitance (C_V) for a given applied voltage (V_R) using the equation[15]

$$C_V = \frac{C_{j0}}{(1 + V_R/V_j)^M} + C_P, \tag{1}$$

where C_{j0} is the zero bias junction capacitance, V_j is the junction potential, M is the grading coefficient, and C_P is the package capacitance. For the specific diode series we have used, these values are $C_{j0} = 2.92$pF, $V_j = 0.68$V, $M = 0.41$, and $C_P = 0.05$pF. The inverse of the square root of the resulting capacitance is shown in Fig. 5(b), as a function of δa. As expected, this plot closely resembles the plots in Fig. 5(a) and Fig. 2. The dependence of the diode capacitance on δa changes the response of the system to linear tuning of the resonant frequencies, since, as discussed earlier, the resonant frequency is dependent on the combined capacitance of the diode, and the SRR.

When the two resonances overlap, it is difficult to accurately distinguish them in the data. Therefore, the experimental values for δa in the shaded regions have been excluded for Figs. 1(c) - 3(a).

In conclusion, we have demonstrated that by shifting two coupled split-ring resonators relative to each other, we can significantly control the nonlinear properties of both the symmetric and antisymmetric resonant modes in the system. We have also found that the tuning of the nonlinear response can be explained and predicted numerically by studying the voltages generated across the

diodes. We expect that our results will stimulate further work in controlling and designing nonlinear properties of metamaterials.

We acknowledge a financial support from the Australian Research Council.

REFERENCES

[1]V.G. Veselago, Sov. Phys. Uspekhi **10**, 5 (1968).
[2]D.R. Smith, W.J. Padilla, D.C. Vier, S.C. Nemat-Nasser, and S. Schultz, Phys. Rev. Lett. **84**, 4184 (2000).
[3]J.B. Pendry, A.J. Holden, D.J. Robbins, and W.J. Stewart, IEEE Trans. Microwave Theory Tech. **47**, 2075 (1999).
[4]T.Q. Li, H. Liu, T. Li, S.M. Wang, F.M. Wang, R.X. Wu, P. Chen, S.N. Zhu, and S. Schultz, Appl. Phys. Lett. **92**, 131111 (2008).
[5]J.B. Pendry, Science **306**, 1353 (2004).
[6]M. Lapine, D.A. Powell, M.V. Gorkunov, I.V. Shadrivov, R. Marques, and Yu.S. Kivshar, Appl. Phys. Lett. **95**, 084105 (2009).
[7]D.A. Powell, K. Hannam, I.V. Shadrivov, and Yu.S. Kivshar, Phys. Rev. B **83**, 235420 (2011).
[8]D.A. Powell, M. Lapine, M.V. Gorkunov, I.V. Shadrivov, and Yu.S. Kivshar, Phys. Rev. B **75**, 155128 (2010).
[9]A. Degiron, J.J. Mock, and D.R. Smith, Opt. Express **15**, 1115 (2007).
[10]M. Lapine, M. Gorkunov, and K.H. Ringhofer, Phys. Rev. E **67**, 065601 (2003).
[11]I.V. Shadrivov, S.K. Morrison, and Yu.S. Kivshar, Opt. Express **14**, 9344 (2006).
[12]D.A. Powell, I.V. Shadrivov, Yu.S. Kivshar, and M.V. Gorkunov, Appl. Phys. Lett. **91**, 144107 (2007).
[13]S. Larouche and D.R. Smith, Opt. Comm. **283**, 1621 (2010).
[14]D. Huang, E. Poutrina, and D.R. Smith, Appl. Phys. Lett. **96**, 104104 (2010).
[15]Skyworks, "Varactor SPICE Models for RF VCO Applications", SMV APN1004 datasheet (2005).